D. L. Demin [*], V. V. Filchenkov, L. N. Generalov [a],
K. I. Gritsaj, A. D. Konin, A. V. Livke [a], A. I. Rudenko,
Yu. I.Vinogradov [a], V. P. Volnykh

GAMMA SPECTROMETER
FOR STUDYING THE MCF REACTIONS

[a] Russian Federal Nuclear Center VNIIEF, Sarov, Russia
[*] E-mail: demin@jinr.ru

Демин Д. Л. и др. E15-2012-107

Гамма-спектрометр для изучения реакций мю-катализа

Рассматривается гамма-спектрометр, состоящий из двух идентичных гамма-детекторов на основе BGO, и соответствующая электроника. Основные характеристики спектрометра: высокая эффективность в диапазоне энергий гамма-квантов $E_\gamma < 30$ МэВ и низкая чувствительность к фону случайных совпадений.

Отличительной особенностью детектора является пластический сцинтиллятор, окружающий кристалл BGO и просматриваемый тем же ФЭУ. Это обеспечивает эффективную защиту BGO-детектора от фона заряженных частиц. Устройство детектора позволяет создать компактную экспериментальную установку с большим телесным углом регистрации гамма-квантов.

Проведено моделирование функции отклика спектрометра на основе программного пакета GEANT-4, которое было проверено экспериментальной калибровкой. Гамма-спектрометр применялся в эксперименте по поиску редкой реакции мю-катализа $dd\mu \rightarrow {}^4\mathrm{He} + \gamma + 23{,}8$ МэВ и предназначен для изучения реакции $pt\mu \rightarrow {}^4\mathrm{He} + \gamma + 19{,}8$ МэВ.

Demin D. L. et al. E15-2012-107

Gamma Spectrometer for Studying the MCF Reactions

A gamma spectrometer composed of two identical BGO-based gamma detectors and associated electronics is described. The main characteristics of the spectrometer are its high detection efficiency in the energy range of gamma rays $E_\gamma \leqslant 30$ MeV and low sensitivity to the accidental background.

A distinctive feature of the detector is a plastic scintillator, which surrounds BGO crystal and is viewed by the same photomultiplier tube. This provides effective protection of the detector against the charged particle background. The detector design allows for a compact experimental setup with a large solid angle of gamma-ray registration.

The simulation of the spectrometer response function has been performed and experimentally verified using GEANT4 program. The spectrometer was used in a search for the rare muon-catalyzed fusion (MCF) reaction $dd\mu \rightarrow {}^4\mathrm{He} + \gamma + 23.8$ MeV and is designed to study the $pt\mu \rightarrow {}^4\mathrm{He} + \gamma + 19.8$ MeV reaction.

INTRODUCTION

Fusion reactions of light nuclei at low energies ($\leqslant 10$ keV) are of interest for nuclear physics of few-nucleon systems, nuclear processes in the Early Universe and the origin of the solar neutrinos [1]. However, experimental studies of these reactions are very complicated.

Coulomb barrier in the entrance channel results in dramatic (near exponential) drop of corresponding cross sections $\sigma(E)$ with decreasing center-of-mass energy E. So, the cross sections for $^2\mathrm{H}(p, \gamma)\,^3\mathrm{He}$ are $\sigma(E = 20 \text{ keV}) \cong 20$ nb and $\sigma(E = 10 \text{ keV}) \cong 2$ nb [2]. Obviously, more efforts should be made for the external (cosmic and possible other) background discrimination to ensure the accurate measurements in this energy range. Both active and passive shielding of the detectors is used for this purpose. The marked improvement in the background conditions was achieved by the LUNA collaboration, which conducts measurements on the 50-keV accelerator in the underground LNGS laboratory [3]. However, even here the influence of electron screening effects complicates the correct data interpretation at low energies.

The phenomenon of muon-catalyzed fusion (MCF) is a successful tool for studying the fusion of hydrogen nuclei in the unique conditions unattainable in "beam-target" experiments [4, 5]. These reactions occur in the vibrational-rotational states of muonic molecules of different types $XX\mu\,(X \equiv p, d, t)$. Due to the small distance between the nuclei ($\simeq 5 \cdot 10^{-11}$ cm), the penetrability of the Coulomb barrier is sufficient for nuclear reaction with a noticeable probability during the muon lifetime $\tau_\mu = 2.2 \ \mu$s.

The structure features of the muonic molecules determine the specific properties of the ongoing reactions:

— ultralow energy of the relative motion of the nuclei (~ 100 eV),

— almost pure wave states of particles (p-wave for the identical nuclei ($X = X$) and s-wave for the different nuclei),

— absence of the distorting effect of the electron screening.

Apart from the above-mentioned, a definite advantage of the method is the use of the signal of the muon-decay electron as a trigger, which sufficiently suppresses the accidental background. So far, most of the MCF reactions have been sufficiently studied experimentally in many laboratories around the world,

including our group. Fusion rates (and, thus, nuclear constants) were measured by various authors for $d + d$ (main channels), $p + d$, and $t + t$ fusion to determine the wave state of the relative motion of nuclei. The following reactions are much less studied:

$$dd\mu \longrightarrow {}^4\text{He}\mu + \gamma + 23.8 \text{ MeV} \quad \text{and} \tag{1}$$

$$pt\mu \longrightarrow {}^4\text{He}\mu + \gamma + 19.8 \text{ MeV}. \tag{2}$$

Process (1) is the most intriguing. Under certain conditions (room temperature), ddμ-molecules are formed mainly in the state, corresponding to almost pure p-wave of relative motion of the nuclei of deuterium [6,7]. The intense E1 transition is sharply suppressed in accordance with the selection rules for parity and isospin. Thus, its intensity appears comparable with a much less intensive M2 transition. As a result, the intensity of the reaction (1) is $10^{-7} - 10^{-6}$ relative to the main dd-fusion channels (${}^2\text{H}(d, {}^3\text{He})n$, ${}^2\text{H}(d, t)H$) [8,9]. As follows from the "beam-target" experiments [10,11], which were carried out with polarized deuteron beam, the reaction $d + d \rightarrow {}^4\text{He} + \gamma$ (40 keV) proceeds giving out gamma rays in different transitions with different statistical weights, namely 55% E2 (s-wave), 29% E1, and 16% M2 (both p-wave). In contrast to this "in-flight" reaction, MCF process (1) is only a p-wave interaction, which gives a new approach for studying the structure of alphaparticles and nuclear dynamics. It should be noted that at the present time, this process is available for *ab initio* theoretical calculations. This makes it important to search for new processes to compare theory with experiment [12]. At present, only our experimental evaluation for the yield of process (1) exists [7]. Further statistical improvement is planned.

Process (2) is interesting because it comes from the s-state of nuclei in M1 transition. It is hardly possible to study it in accelerators, where E1 transition from the p-wave dominates even at low energies [13]. Its yield is expected to reach $\simeq 10^{-2}$ [14]. The only measurements of the yield of the reaction (2), carried out in PSI [15], revealed strong disagreement of the experimental results with the "standard" theory predictions. Obviously, it would be desirable to reproduce this study by an independent experimental method.

Presented gamma spectrometer is designed to study the reactions (1) and (2), proceeding from the state of muonic molecules. It is composed of two identical gamma detectors and related electronics. Because of the low intensity of the studied processes, the detectors must have high detection efficiency ϵ_γ and must be reliably shielded from the ambient (mostly cosmic) background. The final goal of present work is

— to investigate the spectrometric properties of the detectors and to determine ϵ_γ for processes (1) and (2), and

— to achieve a sufficiently low background in the energy range studied.

1. GAMMA DETECTOR

1.1. Design. The gamma detector design is shown in Fig. 1.

The central part of the gamma detector is a BGO crystal ($\oslash 127 \times 60$ mm), which is specially chosen for the detection of gamma rays from reactions (1) and (2). Two BGO crystals were supplied by IIC SB RAS (Novosibirsk) [16]. The sensitive volume of the gamma detector is a "sandwich" (BGO crystal placed in a plastic shell), and is seen by the same photomultiplier tube (PMT) XP4512b.
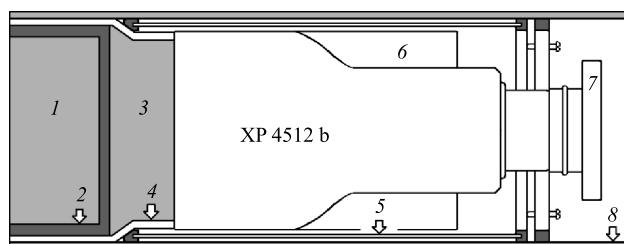
Fig. 1. The gamma detector: *1* — BGO crystal, *2* — plastic scintillator shell, *3* — light-guide, *4* — teflon, *5* — iron magnetic shield, *6* — permalloy magnetic shield, *7* — electronics, *8* — iron casing

The 7-mm-thick plastic scintillator shell, surrounding the BGO crystal, is an active shield against accidental radiation (mainly cosmic muons). Its thickness was chosen [17] so as to effectively detect the background of charged particles and to be insensitive to the secondary radiation leakage from BGO crystal during registration of gamma rays in the above-mentioned reactions. To separate events caused only by scintillation in the BGO crystal (no release of energy in the plastic shell), a fast component and a slow component of the detector signal are compared. Background is discriminated by presence of a sharp difference between the time in plastic scintillation luminescence (several nanoseconds) and in the BGO crystal ≈ 300 ns [18].

We associate the energy of the registered gamma rays with the "charge" of the slow SC component of gamma detector signal, which is the sum of ADC amplitudes of the successive gamma detector signal samples. The value of FC appropriate for the fast component of the gamma detector signal is used for charged particle background discrimination. During the measurements, the BGO crystal is maintained at constant temperature ± 1 °C.

1.2. Spectrometric Properties. The main parameter of the detector is the gamma-ray detection efficiency ϵ_γ. The accuracy and reliability of the measured characteristics of the studied reactions depends on it. The detection efficiency is derived from the detector response function, which is calculated in the traditional way [19] using the GEANT4 program package [20]. When the size of

3

the detector crystal, its elemental composition, and its distance from a point of isotropic monoenergetic gamma source are known, and after the distribution function of the energy absorbed in the detector crystal is calculated, the convolution of this function is performed with the energy resolution function of the detector (a Gaussian function). The calculation of the response function is carried out taking into account the dependence of the absolute energy resolution on the absorbed energy, from its lowest values to the energy values of registered γ-quanta. This calculation method of obtaining the response function has found the convincing evidence in the results of the experimental studies [21] with the simulation of the response functions both carried out by the GEANT4 and MCNP4B codes [22].

At low energy, standard γ-ray sources with known intensity (with an error of 1%), ^{137}Cs (0.662 MeV), ^{60}Co (1.173, 1.333 MeV), ^{88}Y (0.898, 1.836 MeV), and ^{228}Th (2.615 MeV) were used; sources with energies of 2.225 and 4.439 MeV, based on the radiative capture of thermal neutrons $(n + p)$ and the reaction ^{9}Be (α, n) ^{12}C$'$, respectively, were also used. An example of the experimental energy spectrum for ^{88}Y γ-source is shown in Fig. 2.
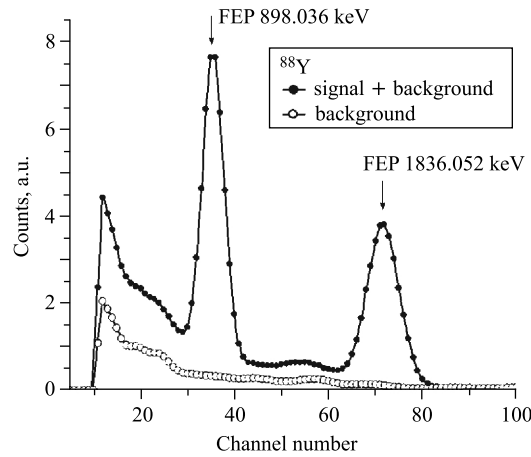
Fig. 2. The energy spectrum for ^{88}Y γ-source: FEP — full-energy peak

Measurements of high-energy gamma rays were performed on an electrostatic tandem accelerator EGP-10 (VNIIEF, Sarov, Russia). Gamma rays were produced by a boron target (6.3% ^{10}B and 93.7% ^{11}B) with the well-known thickness $(1397 \pm 3\%)$ μg/cm^2 exposed to the generator of 4.906-MeV proton beam in the reactions

$$^{11}\text{B}(p, \gamma_0)\, ^{12}\text{C} \quad \text{and} \quad ^{11}\text{B}(p, \gamma_1)\, ^{12}\text{C}'(4.439 \text{ MeV}). \qquad (3)$$
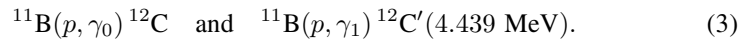
The sum proton flux was equal to $(1.293 \pm 1\%) \cdot 10^{15}$. Gamma rays were detected at an angle of 90° relative to the direction of the proton beam motion.

4

The boron target was located at a distance of 370 mm from the nearest plane of BGO crystal (as well as in the above low-energy measurements). The apparatus spectrum of the gamma rays with average energies $E_{\gamma 0} = (20.433 \pm 0.003)$ MeV and $E_{\gamma 1} = (16.001 \pm 0.003)$ MeV, measured on the accelerator EGP-10 in radiative capture reactions (3), together with the simulation of the spectrum using GEANT4, are shown in Fig. 3.
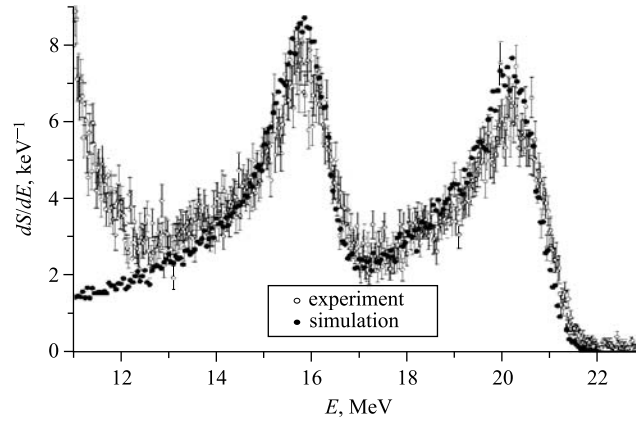
Fig. 3. The energy spectrum of gamma rays $E_{\gamma 0}$ and $E_{\gamma 1}$ from reactions (3): S — partial sum in pulse registration; open circles — measured pulse spectrum vs. pulse amplitudes E; filled circles — simulation using GEANT4

In the region 11.5–12 MeV of the spectrum, a sharp decline is seen, which is a high-energy edge of the peak due to $^{73}\mathrm{Ge}\,(n, \gamma_0)\,^{74}\mathrm{Ge}$ reaction with thermal neutrons. The simulated spectrum was obtained by summing the response functions for γ_0 and γ_1, multiplied, respectively, by the values of relative intensities $I_{\gamma 0} = (4.666 \pm 3.9\%) \cdot 10^6$ and $I_{\gamma 1} = (3.292 \pm 3.9\%) \cdot 10^6$, each of which represents the number of photons emitted (in 4π sr) during proton irradiation by a fictitious isotropic source. These values, of a fictitious source, adequately reflecting the real fall of gamma rays on the BGO crystal [21], were obtained using the absolute differential cross sections for the angle of 90° [23, 24] and the angular distributions [24]. (The gamma-ray sources are fictitiously isotropic only for non-isotropic angular distributions, and are really isotropic for an isotropic angular distribution.)

In the calculation of the response function in its final form, a multiparameter analytical dependence of the detector energy resolution ΔE_γ on the absorbed energy E was used [21]. The full widths at half-height of the full-energy peaks (FEP) helped to carry out this calculation and handle the γ-ray low-energy data (see Fig. 2 for an example). These peaks were used in the energy calibration by determining the dependence of the absorbed energy in the pulse amplitude terms

5

expressed by the channel number of the analyzer. With increasing energy, such a procedure is not possible. Based on simulation results, it has been proven that at the energies higher than 6 MeV, due to higher probability of leaks of one and two annihilation photons and the deterioration of the absolute energy resolution, the isolated FEP ceases to exist. Instead, the asymmetric peak is formed, consisting of unresolved FEP peaks, single and double escape peaks, and the high-energy part of the Compton distribution. For this reason, the high-energy γ-ray energy resolution (as in [19]) and the energy calibration parameters were determined in a process of simulating the experimental spectra.

Let us note an important fact that helps us understand the purpose of the high-energy gamma-ray measurements of the gamma detector. The simulation of the relative energy dependence in the experimental spectrum (Fig. 3) merely means that in the region of a high-energy γ-ray, the energy resolution is found, and the energy calibration of the detector is performed. The coincidence of the experimental and calculated spectra, given in absolute scale, will have to justify the applicability of the simulation method, which is aimed at obtaining the accurate response function and the reliable detection efficiency of high-energy γ-rays. The data in Fig. 3 (GEANT4 code) simply show that the simulation results fit with the experimental data within 4–7%. The MCNP4B code describes the experimental data somewhat better. At low energies, both the GEANT4 and MCNP4B codes reproduce the experimental data equally well. The relative energy resolution with good accuracy can be expressed as

$$\Delta E_\gamma(\%) = 3.9\sqrt{1 + 12/E_\gamma(\text{MeV})}, \tag{4}$$

where the energy E is absorbed in a local process within the BGO crystal and is therefore identified as the energy of registered photons E_γ. For comparison,
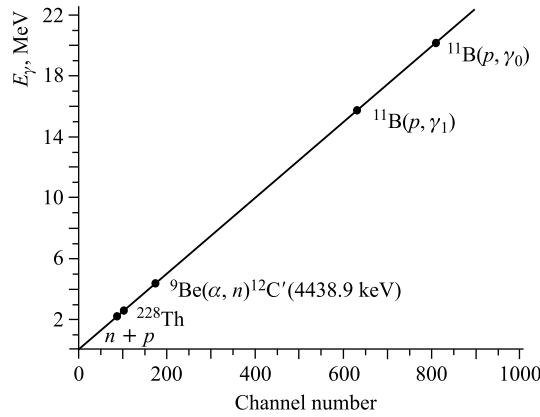
Fig. 4. Data on the energy calibration of the gamma detector

6

we present data for crystals of similar size. In [25], $\Delta E_\gamma \approx 10\%$ for the BGO crystal $\oslash 127 \times 150$ mm at $E_\gamma = 2$ MeV; and in [26], $\Delta E_\gamma = 5-6\%$ for the BGO crystal $\oslash 102 \times 100$ mm at $E_\gamma = 20$ MeV. The appropriate values calculated by the expression (4) are 10.3% and 4.9%.

Figure 4 shows the calibration dependence of the conversion of the absorbed energy in the pulse amplitude (channel number). The characteristics of the gamma-ray sources, indicated along the calibration line, were given in the text.

A transistor high-voltage divider [27] is implemented in the gamma detector, which provides a low level of diffused power and stability of PMT gain. From the description of the experimental data with linear dependence (solid line in Fig. 4), it was found that the conversion is linear within 2%.

1.3. The Charged Particle Background Discrimination. To suppress the charged particle background (cosmic muons), detectors with "external" anticoincidence (AC) are used, which usually complicates installation. At least one external (annular) detector was used with four PMTs [28]. In other cases, more detectors with AC are employed. For example, in [29], two additional cylindrical detectors (each with an angle of $180°$) with eight PMTs were used; in [26], three cylindrical detectors with AC (with an angle of $120°$) were used; and in [29], the latter were used with six PMTs.

In our investigation, we chose the most simple variant, combining the AC plastic and BGO crystal in one detector. For example, this idea was previously realized in experiments with the LAMPF BGO ball spectrometer [30]. It allows a pulse shape discrimination using the fast and slow components (FC-SC) of gamma detector signal. In the two-dimensional FC-SC distribution, the γ-events, registered with the energy deposit only within BGO crystal (no energy deposited
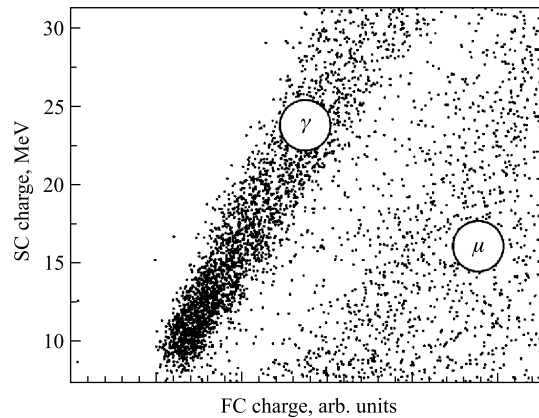
Fig. 5. The two-dimensional FC-SC distribution of the cosmic background (muon and gamma-ray components) obtained with the gamma detector

in the plastic scintillator shell), concentrate in the region of "gamma-branch", which is an area with a certain ratio $SC/FC \simeq 10$. Cosmic muon events, registered in the plastic shell and in the BGO crystal simultaneously, reside in a wide region with a smaller SC/FC ratio (Fig. 5).

Figure 5 illustrates the results of exposition of the gamma detector to cosmic radiation, where the fraction of the registered charged component (cosmic muons), located in the "gamma-branch", does not exceed one tenth of the registered cosmic gamma-ray component. It is very convenient for an experimentalist to distinguish the cosmic gamma rays and cosmic muons within the same device.

Our aim was to investigate the background intensity for $E \leqslant 30$ MeV, where E is the energy deposited within BGO crystal. The gamma detector energy scale was selected as follows. Initially, the maximum amplitude of the signal, corresponding to the ^{60}Co gamma-line maximum energy (2.5 MeV), was installed in the optimal position (2/3 of the full range of amplitude digitizer). After that, the amplitude of the signal from the detector was artificially reduced exactly by a factor of 10. To discriminate the background, we first imposed the limitation on the amplitude of the fast component of the detector signal $FC < FC_{max}$, where $FC_{max} = 2$ MeV, released in the plastic scintillator (appropriate allocation of 60 MeV in BGO crystal), which did exceed the chosen energy range $E_\gamma \leqslant 30$ MeV. Then we selected the events, which were located in the "gamma-branch" on the FC-SC distribution obtained with the gamma detector. The background measurements were performed in the laboratory conditions with and without 5-cm lead shielding. The "open" front of the BGO crystal was further protected by a plastic counter with AC. The results are presented in the table. As seen from the table, the use of the FC-SC criterion reduces the total background intensity by a factor of 3. Obviously, the rest of background mainly consists of cosmic gamma rays. This is confirmed by a significant absorption of external radiation in the 5-cm lead layer.

Cosmic rays measurements in the energy range 10–30 MeV

Variant	Selection based on SC/FC ratio	Passive shielding	Intensity of selected events, $\mathrm{MeV}^{-1} \cdot \mathrm{s}^{-1}$
I	–	–	$4.1 \cdot 10^{-2}$
II	+	–	$1.4 \cdot 10^{-2}$
III	+	5 cm Pb	$2.8 \cdot 10^{-3}$

Comparing the data on variants (I) and (III), we see that even at a relatively low passive shielding, we achieved the background discrimination by a factor of 15. Thus, we can estimate the efficiency of cosmic radiation background suppression in the gamma detector to be at a minimum $\xi = 93-94\%$. The real value of cosmic muon background suppression is estimated from the data on

the gamma-ray attenuation in the lead and the detailed analysis of the FC-SC distribution, and is equal to

$$\xi_\mu \geqslant 99\%. \tag{5}$$

2. THE USE OF THE GAMMA SPECTROMETER IN EXPERIMENT

As mentioned above, we have conducted the first experimental study of the process (1), and are preparing to carry out measurements of the reaction (2). In this Section, we describe the peculiarities of the experimental method. The common important feature of our experimental techniques in the study of muon-catalyzed fusion reactions is to ensure the highest possible ratio of the amount of useful and accidental events. To provide the highest possible effect-to-background ratio, we achieve a compact arrangement of the detectors around the target with the largest possible solid angle covered.

2.1. The Experiment on the $dd\mu \to {}^4\mathrm{He}\,\mu + \gamma$ Process.

2.1.1. The Experimental Geometry and Detection System. The experimental setup for the study of process (1) is shown in Fig. 6. Negative muons from the JINR Phasotron are detected by the beam counters *1–3* and hit the high-pressure deuterium target with an internal volume 275 cm^3 and deuterium pressure of 575 bar. Scintillation counter *4*, surrounding the target, detects muons passing the target without stopping. It also serves as a telescope to detect electrons from the muon decay inside the target, providing a trigger signal. The solid angle for counter *4* was $\Omega_e \simeq 80\%$ (with respect to a full solid angle 4π sr). The number of electrons is used to normalize the number of experimental events.

The main part of the detection system was the gamma spectrometer, which consists of two gamma detectors. Full solid angle for the gamma spectrometer was $\Omega_\gamma \simeq 40\%$. Passive shielding consists of two 5-cm-thick lead layers, which surround the detection system. An additional plastic 1-cm-thick veto counter was placed between these layers above the gamma spectrometer.
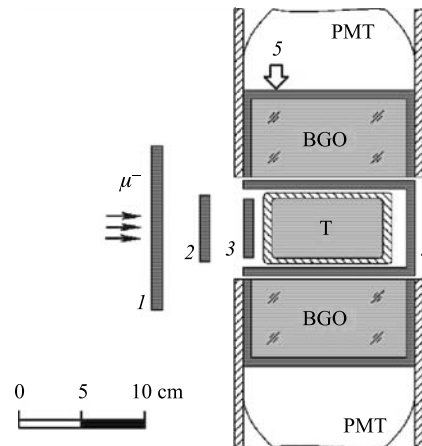
Fig. 6. The experimental setup: *1–4* — muon telescope of plastic counters, *5* — plastic scintillator shell, BGO — scintillation crystal, PMT — photomultiplier, T — target

9

In the previous Section, we studied applicability of simulation to find the detection efficiency. We carried out measurements with the gamma detector at a distance of 370 mm from the source of photons. For gamma rays with energies of ≈ 20 MeV, the choice of a shorter distance (reduced to 70-mm distance used in the experiment) was not possible because of the following: it was complicated and, perhaps, impossible to properly consider big load and the strong Doppler broadening. Moreover, it was problematic to account for the attenuation factors for angular correlations. However, we suppose that if the 370 mm simulation gives correct results, there is no strong reason (edge effects at registration) for the 70-mm simulation to produce incorrect results. The gamma spectrometer response function for the expected from process (1) gamma rays was calculated using the GEANT4-based GAMMA program with the actual geometry of the experiment. The calculation is presented in Fig. 7, which demonstrates that the main energy losses of gamma rays are concentrated within the energy region 15–25 MeV. The peak at lowest energies is mainly due to the Compton backscattering on the materials surrounding BGO crystal.
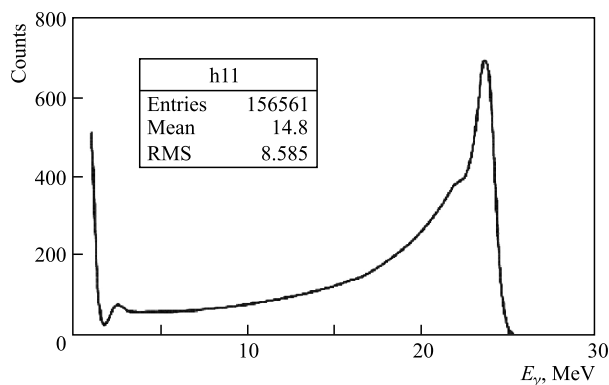
Fig. 7. The calculated response function of the gamma spectrometer for process (1), which corresponds to gamma line $E_\gamma = 23.8$ MeV

The detection efficiency was $\epsilon_\gamma \simeq 24\%$ in the energy range 10–25 MeV, and $\epsilon_\gamma \simeq 15\%$ in the energy range 20–25 MeV. So, we have quite a highly efficient gamma spectrometer, which is important in the study of rare reactions.

2.1.2. The Amplitude and Timing Measurement. The signals from the detection system come to the flash ADC (8 bits $\times$ 2048 samples, 100 Mc/s), thus registering time and sequence of signals. The experimental information from the flash ADC is recorded on a PC for further analysis.

The trigger checks the muon stop signal μ, which is a combination of counter signals $1, 2, 3, \bar{4}$, and the electron signal e (counter *4*) within the interval of 5 and 15 μs before and after the target entry (μ), respectively.

10

For the proper selection of events, we used an experimental method of delayed coincidences $\mu - \gamma - e$, where γ is the signal of the gamma spectrometer. We used a special timing criterion to discriminate the sufficient background due to stops of muons and electrons in the target walls, and, thus, reduced the number of registered accidental counts [7]. This caused the relative loss in gamma-ray detection efficiency by a factor of $f_t = 0.4$.

2.1.3. The Results of the Experiment. Overall energy spectrum of experimental events, which satisfies all the selection criteria for the gamma rays, is shown in Fig. 8.
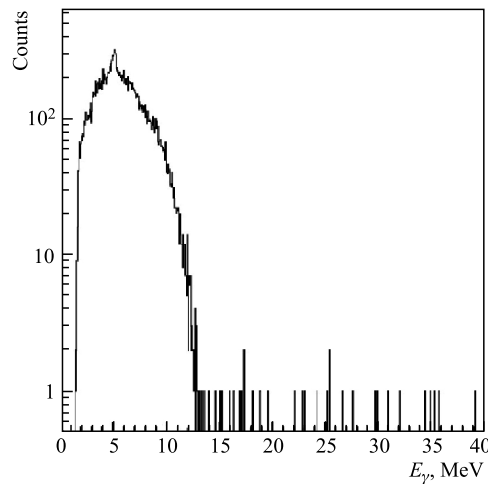
Fig. 8. The experimental gamma-ray energy spectrum registered with the gamma spectrometer

The figure shows an intense gamma-ray "bump" in the $E_\gamma \leqslant 12$ MeV region. This region is related to the $n-\gamma$ reactions on iron (in the walls of the target), caused by neutrons with an energy of 2.5 MeV from the $dd\mu \rightarrow {}^3\mathrm{He}\,\mu + n + 3.3$ MeV process. On the top of the "bump", one can see a weak peak at $E_\gamma = 5.5$ MeV. This peak is caused by the $d\mu + p \rightarrow pd\mu \rightarrow {}^3\mathrm{He}\,\mu + \gamma + 5.5$ MeV reaction, which occurs at a low concentration of protium (1%) in deuterium. This reaction was used as an additional verification tool of the gamma spectrometer calibration. In total, we accumulated $N_e = 4 \cdot 10^7$ electrons from the decay of muons stopped in deuterium, which corresponds to $n_{dd\mu} = 10^8$ cycles of $dd\mu$ formation. Four events $n_{\mathrm{reg}} = 4$ were registered in the energy range 20–25 MeV.

The background was estimated by means of the analysis [7]. It was found that the component of the background associated with the muon beam (correlated background) should be $n_b^{\mathrm{corr}} = 1.4 \pm 0.2$, and the accidental counts were $n_b^{\mathrm{acc}} =$

2.6 ± 0.4. Thus, the total number of expected background counts equals $n_b = 4 \pm 0.6$. As a result, all the events can be explained by background processes. So, we have given only an estimation of the partial yield of the process $\eta_\gamma = (dd \rightarrow {}^4\text{He} + \gamma)/(dd \rightarrow {}^3\text{He} + n; t + p) \leqslant 8 \cdot 10^{-7}$ at a confidence level of 90%. This order of magnitude was expected from the results of [11] obtained in the collision experiments with beams. Achieved in [7], the sensitivity is

$$\alpha = n_b/[(\epsilon_\gamma f_t)\, n_{dd\mu}] = (6-8) \cdot 10^{-7} \qquad (6)$$

The value in (5), obtained for the suppression of the cosmic muon background, makes it possible to conclude that under experimental condition with optimal shielding, the sensitivity level of $\alpha \simeq 10^{-7}$ can be achieved. This will advance the study of process (1) and reliably measure its yield with increasing experimental statistics by one to two orders of magnitude.

2.2. The Study of $pt\mu \rightarrow {}^4\text{He}\,\mu + \gamma$ **Process.** This project is currently under implementation. The experimental setup is similar to the one used to study the reaction (1) (Fig. 6), except for the target. The new target will have a volume of 50 cm^3. It will contain liquid H/T mixture (1% T 99% H) at temperature 22 K. The same gamma spectrometer will be used. The calculated gamma spectrometer response function for the gamma line $E_\gamma = 19.8$ MeV is shown in Fig. 9.
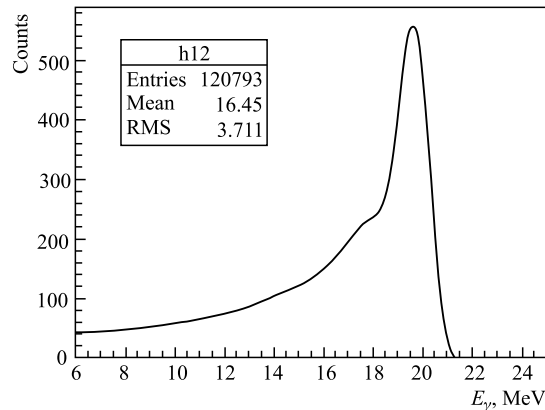
Fig. 9. The calculated gamma spectrometer response function for process (2), which corresponds to gamma line $E_\gamma = 19.8$ MeV

It was calculated using the same Monte Carlo program, which was used in the above experiment. The new experimental geometry was also taken into account. The overall detection efficiency for 19.8-MeV gamma rays was close to 24%. The specific efficiencies 20% and 15% corresponded to the energy deposit thresholds of 10 and 15 MeV, respectively. This high efficiency yields

12

complete statistics of the registered γ-events, which helps to show whether the theory [14] or experiment [15] is correct. Based on experimental data [15], we expect to register $\simeq 2 \cdot 10^5$ γ-events of process (2) within the data taking period (100 hours) at the JINR Phasotron. If the theory [14] is correct, the collected statistics will be eight times less.

CONCLUSION

The gamma spectrometer is described. It is designed to study muon-catalyzed fusion reactions, yielding high-energy gamma rays (≈ 20 MeV). Two identical BGO-based gamma detectors with the inner anticoincidence plastic scintillator shell were used in the spectrometric system. The spectrometric characteristics of the gamma detector were experimentally measured in a wide energy range 0.6–20 MeV and confirmed in simulations using the GEANT4 and MCNP4B software packages. The gamma spectrometer response function for gamma rays, peculiar to the geometry of the experiment, was calculated using GEANT4-based GAMMA program. The compact geometry of the gamma spectrometer provided high detection efficiency, $\epsilon_\gamma = 15-20\%$. The significant background suppression and the usage of the gamma spectrometer allowed us to obtain experimental sensitivity in a search for the deuteron radiative capture from the p-wave state of deuteron muonic molecule (1) at a level of $7 \cdot 10^{-7}$; it also confirmed the predictions of very low intensity of this process in an experiment.

REFERENCES

1. L. E. Marcucci, et al., Nucl. Phys. A 777 (2006) 111.
2. C. Casella, et al., Nucl. Phys. A 706 (2002) 203.
3. U. Greife, et al., Nucl. Instr. Meth. A 350 (1994) 327;
   M. Junker, et al., Phys. Rev. C 57 (1998) 2700.
4. J. D. Jackson, Phys. Rev. 106 (1957) 330.
5. Ya. B. Zeldovich, S. S. Gershtein, Sov. Phys. Usp. 3 (1961) 593.
6. L. N. Bogdanova, V. V. Filchenkov, Hyp. Int. 138 (2001) 321.
7. V. V. Baluev, et al., J. Exp. Theor. Phys. 113 (2011) 68.
8. C. A. Barnes, et al., Phys. Lett. B 197 (1987) 315.
9. F. J. Wilkinson, F. E. Cecil, Phys. Rev. Lett. C 31 (1985) 2036.
10. L. H. Kramer, et al., Phys. Lett. B 304 (1993) 208.
11. K. Sabourov, et al., Phys. Rev. C 70 (2004) 064601.

12. A. Deltuva, A. C. Fonseca, Phys. Rev. C 81 (2010) 054002.

13. R. S. Canon, et al., Phys. Rev. C 65 (2002) 044008.

14. L. N. Bogdanova, V. E. Markushin, Nucl. Phys. A 508 (1990) 29c.

15. P. Baumann, et al., Phys. Rev. Lett. 70 (1993) 3720;
    F. J. Hartmann, et al., Hyp. Int. 82 (1993) 259.

16. V. A. Gusev, et al., Nucl. Instr. Meth. A 460 (2001) 457.

17. V. P. Volnykh // Proc. of the MCF-07 Conf., Dubna, 2008, p. 397.

18. M. Moszynski, et al., Nucl. Instr. Meth. 188 (1981) 403.

19. M. Taiuti, et al., Nucl. Instr. Meth. A 211 (1983) 135.

20. S. Agosninelly, et al., Nucl. Instr. Meth. A 506 (2003) 250.

21. L. N. Generalov, et al., Preprint of Russian Federal Nuclear Center VNIIEF, Sarov, Russia, No. 104-2009 (2009) 51.

22. Documentation for CCC-660/MCNP4B2 Code Package, Contributed by Transport Methods Group LANL, J.F. Briesmeister (Ed.). Los Angeles, 1997.

23. M. C. Wright, et al., Phys. Rev. C 25 (1982) 2823.

24. M. T. Collins, et al., Phys. Rev. C 26 (1982) 332.

25. E. R. van der Graaf, et al., Nucl. Instr. Meth. A 575 (2007) 507.

26. P. Corvisiero, et al., Nucl. Instr. Meth. A 294 (1990) 478.

27. V. A. Kalinnikov, et al., Instr. Exp. Tech. 49 (2006) 223.

28. D. J. Wagennar, et al., Nucl. Instr. Meth. A 234 (1985) 109.

29. M. Anghinolfi, et al., Nuovo Cimento 77A (1983) 277.

30. E. A. Pasyuk, et al., Phys. Rev. C 55 (1997) 1026.

Редактор *С. В. Савиных*